

# Performance Analysis of DS/CDMA Systems with Shadowing and Flat Fading

Jack W. Stokes\*

Microsoft Research  
Signal Processing Group  
One Microsoft Way  
Redmond, WA 98052  
(425)-703-1993  
jstokes@microsoft.com

James A. Ritcey

Department of Electrical Engineering  
University of Washington, Box 352500  
Seattle, WA 98195-2500  
(206)-543-4702  
ritcey@ee.washington.edu

October 17, 2007

---

\*Contact Author.



# Performance Analysis of DS/CDMA Systems with Shadowing and Flat Fading

Jack W. Stokes

Microsoft Research, One Microsoft Way, Redmond, WA 98052

James A. Ritcey

Department of Electrical Engineering, University of Washington

Box 352500, Seattle, WA 98195-2500

*Key Words:* DS/CDMA; shadowing; fading; saddle point integration; numerical contour integration; Padé approximation.

## Abstract

A new method is developed for evaluating the error probability ( $P_e$ ) for Direct Sequence, Code Division Multiple Access (DS/CDMA) wireless systems that includes the effects of shadowing and fading. The method is based on saddle point integration (SPI) of the test statistic's moment generating function (MGF) in the complex plane. The SPI method is applicable to both ideal and wireless channels. For wireless channels, a Padé approximation (PA) of the MGF, which is derived from the moments of the channel's shadowing and fading distributions, allows efficient evaluation of the  $P_e$ . The SPI method can be used to model independent channels using separate shadowing and fading moments for each individual channel. The relative error between the probability density function (PDF) of the composite variate representing log-normal shadowing and Rayleigh fading and the PDF found from the inverse Laplace transform of the PA is negligible. Results show that log-normal shadowing increases the  $P_e$  by 100% to 1000% compared to channels exhibiting fading only.

## 1 Introduction

Much research effort has been directed towards the performance evaluation of Direct Sequence, Code Division Multiple Access (DS/CDMA) communication systems during the past two decades. Methods for computing the error probability,  $P_e$ , for DS/CDMA systems have been proposed for both ideal channels [14], [13], [16], [18], and fading channels [3], [4].

Recently, DS/CDMA models have been improved to include the effects of channel coding and multiuser receivers [10], [11], [12]. It is well known that wireless channels are affected by shadowing, which is a long-term variation in the mean envelope averaged over several wavelengths, in addition to fading [17]. Due to the mathematical complexity, previous methods for computing the  $P_e$  for wireless channels have not included the effects of both shadowing and fading. In this paper, we develop a new method for evaluating error probabilities for DS/CDMA wireless systems including the effects of shadowing as well as flat fading. In the process, we also present the method for ideal channels.

Saddle point integration (SPI) is used to efficiently evaluate chip-asynchronous, DS/CDMA error probabilities. SPI is based on numerical contour integration of the test statistic's moment generating function (MGF) in the complex plane. The SPI method has been used to compute the error probability resulting from intersymbol and cochannel interference [6], radar detection probabilities [7], and K-distributions [5]. SPI is superior to the characteristic function method presented in [3] because it is less susceptible to roundoff error due to the integrand oscillations, and this property is particularly valuable for automated system modeling tools.

We use Padé approximations (PAs) [1] [2] to model the effects of shadowing and flat fading channels. The unconditioned MGF, averaged over the shadowing and fading distributions, is approximated by its PA. This PA is determined from the moments of the shadowing and fading distributions. In this work, we consider mean envelope, log-normal shadowing as well as Rayleigh and Ricean fading. However, the model is applicable to any channel given the exact moments of the shadowing and fading distributions. The SPI method is completely general and does not place any restrictions on the channel statistics. Independent channels can be modeled using separate shadowing and fading moments for each individual channel. As a result, one can model different types of channels simultaneously such as Rayleigh fading with shadowing and Ricean fading without shadowing.

Previous results in the literature have considered the average  $P_e$  based on the statistics of the source, channel, and additive white Gaussian noise (AWGN). However, the systems engineer must also determine the worst case  $P_e$  when analyzing a wireless communication system for a particular environment. For the reverse link from the mobile station (MS) to the base station (BS), we compare the average and worst case  $P_e$  given rectangular chips where the average  $P_e$  is determined by modeling the multiple access interference (MAI) sources with asynchronous chips while the worst case  $P_e$  is found assuming synchronous chips for the MAI sources. This analysis does not apply to the forward link from the BS to the MS in cellular DS/CDMA, which is also synchronous, because the separate information sequences are spread at the BS with orthogonal, Walsh-Hadamard sequences prior to transmission.

This paper is organized as follows. In section 2, we present the chip-asynchronous DS/CDMA system model. The SPI method is derived for random signature sequences for ideal channels in section 3 and wireless channels with shadowing and fading in section 4. Finally in section 5, we present numerical results which evaluate the error probabilities for all channel models.

## 2 System Model

Consider  $l = 0, 1, \dots, L$  co-channel, DS/CDMA sources where each source transmits with a periodic code of length/period  $N$ . For a chip period of  $T_c$ , the resulting symbol rate is  $1/T$  with  $T = NT_c$ . The baseband signal transmitted by the  $l^{th}$  source is

$$s_l(t) = a_l \sum_{k=-\infty}^{\infty} i_l[k] h_l(t - kT) \quad (1)$$

where  $a_l$  is the transmitted signal amplitude,  $i_l[k] \in \{+1, -1\}$  is the equally likely, information symbol modulated using binary phase shift keying (BPSK), and  $h_l(t)$  is the chip

sequence

$$h_l(t) = \sum_{n=0}^{N-1} b_l[n]p(t - nT_c). \quad (2)$$

The signature sequence,  $\mathbf{b}_l = [b_l[0], \dots, b_l[N-1]]^T$ ,  $b_l[k] \in \{+1, -1\}$ , specifies the pseudo noise (PN) sequence employed by the  $l^{\text{th}}$  transmitter to spread the information symbol. The chip waveform,  $p(t)$ , is supported on the interval  $[0, T_c]$  and has normalized energy,  $\int_0^{T_c} p^2(t)dt = 1$ .

The signal from each source is transmitted over an ideal or wireless channel, and the sum of the reference signal ( $l = 0$ ) and MAI signals ( $l = 1, \dots, L$ ) is also corrupted with AWGN. The amplitude attenuation introduced by the channel from the  $l^{\text{th}}$  transmitter to the reference receiver is  $\alpha_l$ , while  $\theta_l$  represents the phase offset. The received baseband signal for a chip-asynchronous DS/CDMA system model is

$$r(t) = a_0\alpha_0 \sum_{k=-\infty}^{\infty} i_0[k]h_0(t - kT) + \sum_{l=1}^L a_l\alpha_l \cos(\theta_l) \sum_{k=-\infty}^{\infty} i_l[k]h_l(t - kT - \epsilon_l) + w(t). \quad (3)$$

The first term is the desired signal, the second term is the MAI noise produced by the  $L$  additional transmitters, while the last term is AWGN with zero mean and power density  $N_0/2$ . In our work, we assume perfect phase coherence ( $\theta_0 = 0$ ) and chip synchronization ( $\epsilon_0 = 0$ ) for the reference source, and random phase coherence ( $\theta_l$ ) and chip offsets ( $\epsilon_l$ ) for each of the MAI sources. The reference receiver in figure 1 is a continuous-time matched filter, matched to the transmitter's chip pulse, followed by a discrete-time correlator that correlates the output of the matched filter with the reference receiver's signature sequence. Without loss of generality, assume that the current information symbol sent by the reference transmitter,  $i_0[k]$ , is +1. The test statistic for the signal received from the  $l^{\text{th}}$  source with asynchronous chips is

$$z_l = a_l\alpha_l \cos(\theta_l)\beta_l. \quad (4)$$

Assuming  $p(t)$  is rectangular, the random variable  $\beta_l$ , which represents the cross-correlation

between the signature sequences of the  $l^{\text{th}}$  MAI source and the reference source, is

$$\begin{aligned}
\beta_l &= \tau_l \left\{ \sum_{n=0}^{j_l} i_l[k-1] b_l[n-j_l-1] b_0[n] + \sum_{n=j_l+1}^{N-1} i_l[k] b_l[n-j_l-1] b_0[n] \right\} + \\
&\quad (1-\tau_l) \left\{ \sum_{n=0}^{j_l-1} i_l[k-1] b_l[n-j_l] b_0[n] + \sum_{n=j_l}^{N-1} i_l[k] b_l[n-j_l] b_0[n] \right\} \\
&= \tau_l \left\{ \sum_{n=0}^{j_l} \zeta_{l,n,1} + \sum_{n=j_l+1}^{N-1} \gamma_{l,n,1} \right\} + (1-\tau_l) \left\{ \sum_{n=0}^{j_l-1} \zeta_{l,n,2} + \sum_{n=j_l}^{N-1} \gamma_{l,n,2} \right\} \tag{5}
\end{aligned}$$

where  $\epsilon_l = (j_l + \tau_l)T_c$ ,  $j_l$  is the discrete, random code offset,  $\tau_l$  is the normalized chip offset uniformly distributed over  $[0, 1]$ , and  $b_l[n - j_l] = b_l[N + n - j_l]$  for  $n - j_l < 0$ . In this paper, we choose to model random signature sequences where the chips are equally likely with  $b_l[n] \in \{+1, -1\}$ . With equally likely MAI information symbols and random signature sequences, the intermediate values  $\zeta_{l,n,1}$ ,  $\gamma_{l,n,1}$ ,  $\zeta_{l,n,2}$ , and  $\gamma_{l,n,2}$  are iid binary random variables equally likely to assume values  $(\pm 1)$ . To model MAI sources with synchronous chips, we set  $\theta_l = 0$  and  $\tau_l = 0$  such that  $z_l = a_l \alpha_l \{ \sum_{n=0}^{j_l-1} \zeta_{l,n,2} + \sum_{n=j_l}^{N-1} \gamma_{l,n,2} \}$ . With this chip asynchronous model and independent sources, we can analyze the reverse link. The model is easily extended to the forward link by considering the sum of multiple, chip synchronous sources being transmitted over a single channel to the receiver.

### 3 Ideal Channels

Before considering the more difficult case of wireless channels, we first derive an expression for the  $P_e$  using the SPI method for a DS/CDMA system with ideal channels where the channel attenuation,  $\alpha_l$ , is deterministic. For this system model with  $L$  MAI sources, the probability of error is given by

$$P_e = Pr(r = z_0 + \sum_{l=1}^L z_l + w < 0 \mid i_0[k] = +1) = \int_{-\infty}^0 p(r) dr \tag{6}$$

where  $r$  and  $w$  are the test statistics of the received signal and the AWGN, respectively, and  $p(r)$  is the probability density function (PDF) of  $r$ . In order to avoid difficulties in evaluating

the PDF of the MAI, the SPI method calculates the  $P_e$  from the MGF of  $r$  along a suitable contour in the complex plane. Since  $z_0$ ,  $z_l$ , and  $w$  in (6) are independent, the MGF of  $r$ , as defined in [6], is

$$H(u) = E\{e^{-ru}\} = \int_{-\infty}^{\infty} e^{-ru} p(r) dr = \gamma(u) \prod_{l=1}^L \eta_l(u) H_w(u) \quad (7)$$

where  $\gamma(u)$ ,  $\eta_l(u)$ , and  $H_w(u)$  represent the MGFs of the reference signal, the  $l^{\text{th}}$  MAI signal and the Gaussian noise, respectively. The  $P_e$  can be recovered using (6) and the inverse Laplace transform of  $H(u)$  yielding

$$P_e = \int_{C^\mp} u^{-1} H(u) \frac{du}{2\pi j} + \begin{cases} 1 & \text{conditioned upon } i_0[k] = -1 \\ 0 & \text{conditioned upon } i_0[k] = +1 \end{cases} \quad (8)$$

where  $j = \sqrt{-1}$  and  $C+$  ( $C-$ ) is a vertical contour in the complex  $u$  plane that crosses the real  $u$  axis in the right (left) half plane. Conditioned upon  $i_0[k] = -1$ , the contour integral in (8) evaluates to a result between -1.0 and 0.0 producing a value for the  $P_e$  between 0.0 and 1.0.

Next, we derive the MGFs for the reference signal, an individual MAI signal, and the AWGN in order to evaluate the  $P_e$  given in (8). Because we assume perfect synchronization to the reference signal,  $z_0$  is deterministic, and we find  $\gamma(u) = E\{\exp(-uz_0)\} = \exp(-ua_0\alpha_0N)$ . The MGF of an MAI signal is

$$\eta_l(u) = E\{\exp(-uz_l)\} = E\{e^{-ua_l\alpha_l \cos(\theta_l)\beta_l}\}. \quad (9)$$

Given the independence of  $\zeta_{l,n,1}$ ,  $\zeta_{l,n,2}$ ,  $\gamma_{l,n,1}$ , and  $\gamma_{l,n,2}$  in (5), for fixed  $n$  as well as the independence of these bivariate random variables along index  $n$ , the MGF of the  $l^{\text{th}}$  MAI signal is

$$\begin{aligned} \eta_l(u) &= E\{\exp(-ua_l\alpha_l \cos(\theta_l) (\tau_l \{ \sum_{n=0}^{j_l} \zeta_{l,n,1} + \sum_{n=j_l+1}^{N-1} \gamma_{l,n,1} \} + (1 - \tau_l) \{ \sum_{n=0}^{j_l-1} \zeta_{l,n,2} + \sum_{n=j_l}^{N-1} \gamma_{l,n,2} \} ))\} \\ &= E_{\tau_l, \theta_l} \left\{ \prod_{n=0}^{j_l} E_{\zeta_{l,n,1}} \{ \exp(-ua_l\alpha_l \cos(\theta_l) \tau_l \zeta_{l,n,1}) \} \right\} \end{aligned}$$

$$\begin{aligned}
& \prod_{n=j_l+1}^{N-1} E_{\gamma_{l,n,1}} \{ \exp(-ua_l \alpha_l \cos(\theta_l) \tau_l \gamma_{l,n,1}) \} \\
& \prod_{n=0}^{j_l-1} E_{\zeta_{l,n,2}} \{ \exp(-ua_l \alpha_l \cos(\theta_l) (1 - \tau_l) \zeta_{l,n,2}) \} \\
& \prod_{n=j_l}^{N-1} E_{\gamma_{l,n,2}} \{ \exp(-ua_l \alpha_l \cos(\theta_l) (1 - \tau_l) \gamma_{l,n,2}) \} \\
= & E_{\tau_l, \theta_l} \{ \cosh(u\alpha_l A)^{j_l+1} \cosh(u\alpha_l A)^{N-j_l-1} \cosh(u\alpha_l B)^{j_l} \cosh(u\alpha_l B)^{N-j_l} \} \\
= & E_{\tau_l, \theta_l} \{ (\cosh(u\alpha_l A) \cosh(u\alpha_l B))^N \} \tag{10}
\end{aligned}$$

where  $A = a_l \cos(\theta_l) \tau_l$  and  $B = a_l \cos(\theta_l) (1 - \tau_l)$  for rectangular chips. The MGF of the noise test statistic is  $H_w(u) = \exp(\frac{1}{2} \sigma_w^2 u^2)$  where  $\sigma_w^2$  is the variance of the AWGN.

To minimize round off error given that the MGF is symmetric about the real  $u$  axis, we follow Helstrom and Ritcey [7] and rewrite the integral in (8) as

$$P_e = \int_{c-j\infty}^{c+j\infty} e^{\Phi(u)} \frac{du}{2\pi j} \tag{11}$$

where the ‘‘phase’’ is  $\Phi(u) = \ln(u^{-1} H(u))$ . Substituting the MGFs, the phase for random signature sequences received over ideal channels is given by

$$\Phi(u) = \sum_{l=1}^L \ln(E_{\tau_l, \theta_l} \{ (\cosh(u\alpha_l A) \cosh(u\alpha_l B))^N \}) + \frac{1}{2} \sigma_w^2 u^2 - a_0 \alpha_0 N u - \ln u. \tag{12}$$

The Bromwich contour in (11) is chosen to cross the real  $u$  axis at the saddle point,  $u_0$ , where  $\Phi'(u_0) = 0$ . We use Newton-Raphson to numerically determine the saddle point. The first and second derivatives of the phase, which are required for the Newton-Raphson calculation, are

$$\begin{aligned}
\Phi'(u) &= N \sum_{l=1}^L E_{\tau_l, \theta_l} \{ (\alpha_l A) \tanh(u\alpha_l A) + (\alpha_l B) \tanh(u\alpha_l B) \} + \sigma_w^2 u - a_0 \alpha_0 N - u^{-1} \\
\Phi''(u) &= N \sum_{l=1}^L E_{\tau_l, \theta_l} \{ (\alpha_l A)^2 \operatorname{sech}(u\alpha_l A) + (\alpha_l B)^2 \operatorname{sech}(u\alpha_l B) \} + \sigma_w^2 + u^{-2}. \tag{13}
\end{aligned}$$

For ideal channels, we evaluate  $E_{\tau_l, \theta_l} \{ \}$  in (12) and (13) numerically by averaging uniformly over  $0 \leq \tau_l < 1$  and  $0 \leq \theta_l < 2\pi$ .

Relocating the contour to the saddle point, the probability of error becomes

$$P_e = \int_{u_0-j\infty}^{u_0+j\infty} e^{\Phi(u)} \frac{du}{2\pi j}. \quad (14)$$

From Rice [15], we use the trapezoidal rule which is best for infinite integrals of analytic functions to numerically compute the integral in (14). The initial step size in the trapezoidal integration is chosen to be  $\Delta v = (2/\Phi''(u_0))^{1/2}$  where the step size is halved until the difference between the last two  $P_e$  estimates is less than some prescribed error tolerance. This error tolerance determines the accuracy and efficiency of the algorithm. Bounds on the truncation error can be developed by applying the results of the appendix in [6].

## 4 Wireless Channels With Shadowing and Flat Fading

Next, we extend the results for ideal channels from the previous section to wireless channels. To model the random effects of wireless channels, we replace the deterministic attenuation with a product of random variables,  $\alpha_l = \Omega_l R_l$ , where  $\Omega_l$  and  $R_l$  represent the shadowing and flat fading, respectively. As a result, we must re-evaluate the MGFs for the reference signal,  $\gamma(u)$ , and the MAI signals,  $\eta_l(u)$ , where the "expectation" in the MGF is now taken with respect to the shadowing and fading distributions in addition to the chip and phase offsets.

### 4.1 Reference Signal

For the reference signal, the unconditioned MGF for a wireless channel is

$$\begin{aligned} \gamma(u) &= E_{\Omega_0 R_0} \{ \exp(-ua_0 \Omega_0 R_0 N) \} \\ &= \int_0^\infty \int_0^\infty \exp(-ua_0 \Omega_0 R_0 N) p_{\Omega_0}(\Omega_0) p_{R_0}(R_0) d\Omega_0 dR_0. \end{aligned} \quad (15)$$

A closed form expression for this term cannot be derived for the combined effects of shadowing and fading. This motivates a more general approach based on the Padé approximation (PA)

technique. The  $[M_N/M_D]$  PA is a rational approximation of the MGF with numerator order  $M_N$  and denominator order  $M_D$ . We apply a PA of the MGF constructed by matching the moments of the shadowing and fading statistics [1] [2]. This PA technique is absolutely critical to the development of an efficient, general purpose evaluation for wireless channels. For each system configuration, the PA for the reference signal is computed only once. Thus, the method is computationally efficient since the MGF can then be rapidly evaluated for any complex  $u$ . The PA is determined after expanding the exponential in (15),

$$\begin{aligned} E_{\Omega_0 R_0} \{ \exp(-ua_0 \Omega_0 R_0 N) \} &= \sum_{k=0}^{\infty} \frac{(-ua_0 N)^k}{k!} E\{\Omega_0^k\} E\{R_0^k\} \\ &= \sum_{k=0}^{\infty} \frac{(-ua_0 N)^k}{k!} \mu_{\Omega_0}^{(k)} \mu_{R_0}^{(k)} \end{aligned} \quad (16)$$

where  $\mu_{\Omega_0}^{(k)}$  and  $\mu_{R_0}^{(k)}$  are the  $k^{th}$  moments of reference channel's shadowing and fading distributions, respectively. For the reference signal,

$$\sum_{k=0}^{\infty} \frac{(-ua_0 N)^k}{k!} \mu_{\Omega_0}^{(k)} \mu_{R_0}^{(k)} = P_0(u) + O(u^{M_N+M_D+1}) \quad (17)$$

where the  $[M_N/M_D]$  PA,  $P_0(u)$ , is

$$P_0(u) = \frac{g_0 \prod_{i=1}^{M_N} (u - z_{0,i})}{\prod_{j=1}^{M_D} (u - p_{0,j})}. \quad (18)$$

In (18),  $g_0$  is the overall gain, and  $z_{0,i}$  and  $p_{0,j}$  are the  $i^{th}$  zero and  $j^{th}$  pole, respectively, for the PA of reference signal 0.

## 4.2 Shadowing

To compute the PA in (17), we first need to determine the moments of the shadowing distribution. We assume mean envelope shadowing in (17) by modeling the mean envelope as a log-normal variate [17]. A log-normal variate,  $\Omega$ , is given by  $\Omega = 10^{X/10} = e^{\xi X}$  where  $\xi = \log_e(10)/10$  and  $X$  is normal,  $N(\mu_X, \sigma_X)$ . The PDF of  $\Omega$  is

$$p(\Omega) = \frac{1}{\xi \Omega \sigma_X \sqrt{2\pi}} \exp(- (10 \log_{10}(\Omega) - \mu_X)^2 / (2\sigma_X^2)) \quad (19)$$

with moments

$$\mu_{\Omega}^{(k)} = E\{\Omega^k\} = E\{\exp(\xi X k)\} = \exp(k\xi\mu_X + (\xi k\sigma_X)^2/2). \quad (20)$$

### 4.3 Flat Fading

The evaluation of the PA in (17) also requires the moments of the fading distribution. For Rayleigh fading with Gaussian variance  $\sigma^2$ , the PDF for  $R \geq 0$  is

$$p(R) = \frac{R}{\sigma^2} \exp(-R^2/2\sigma^2) \quad (21)$$

and the moments are

$$\mu_R^{(k)} = (2\sigma^2)^{\frac{k}{2}} \Gamma(1 + \frac{k}{2}). \quad (22)$$

The Gamma function,  $\Gamma(p)$ , is defined for  $p > 0$  as  $\Gamma(p) = \int_0^\infty t^{p-1} e^{-t} dt$  with  $\Gamma(1/2) = \sqrt{\pi}$  and  $\Gamma(3/2) = \sqrt{\pi}/2$ . When  $p$  is an integer,  $\Gamma(p) = (p-1)!$ .

Likewise for Ricean fading with specular parameter,  $s$ , and Gaussian variance  $\sigma^2$ , the PDF for  $R \geq 0$  is

$$p(R) = \frac{R}{\sigma^2} \exp(-(R^2 + s^2)/2\sigma^2) I_0(\frac{Rs}{\sigma^2}) \quad (23)$$

where  $I_0(p)$  is the modified Bessel function of order zero defined for  $p \geq 0$  as

$$I_0(p) = \sum_{k=0}^{\infty} \frac{(p/2)^{2k}}{k! \Gamma(k+1)}. \quad (24)$$

We compute the moments for Ricean fading,  $\mu_R^{(k)}$ , using the efficient recursion from Helstrom [8].

### 4.4 MAI Signals

Like the reference signal, each MAI signal is independent and subjected to shadowing and flat fading. Setting  $\tau = \tau_l$ ,  $\theta = \theta_l$ ,  $\Omega = \Omega_l$  and  $R = R_l$ , the MGF for each MAI signal in (10)

is

$$\eta_l(u) = E_{\tau,\theta,\Omega,R}\{(\cosh(u\Omega RA) \cosh(u\Omega RB))^N\}. \quad (25)$$

To evaluate (25), we must symbolically raise the "cosh" to a power,

$$\begin{aligned} (\cosh(u\Omega RA) \cosh(u\Omega RB))^N &= \left[ \frac{1}{2} \cosh(ua \cos(\theta)\Omega R) + \frac{1}{2} \cosh(ua \cos(\theta)\Omega R(1 - 2\tau)) \right]^N \\ &= \left[ \frac{1}{2} \sum_{k=0}^{\infty} \frac{(ua \cos(\theta)\Omega R)^{2k} (1 + (1 - 2\tau)^{2k})}{(2k)!} \right]^N \\ &= \left[ \sum_{k=0}^{\infty} w_{2k} (u\Omega R)^{2k} \right]^N = \sum_{k=0}^{\infty} v_{2k} (u\Omega R)^{2k} \end{aligned} \quad (26)$$

where  $w_{2k}$  is an intermediate variable and Miller's algorithm [2], [9] is used to evaluate the desired resulting coefficients,  $v_{2k}$ . Miller's algorithm is an efficient method for raising a polynomial,  $f(z) = \sum_{n=0}^{\infty} c_n z^n$ , to an integer power,  $W(z) = [f(z)]^k = \sum_{n=0}^{\infty} v_n z^n$ , by setting  $v_0 = c_0 = 1$  and computing

$$v_n = \frac{1}{n} \sum_{m=1}^n [(k+1)m - n] c_m v_{n-m} \quad n = 1, 2, \dots \quad (27)$$

Substituting (26) into (25) gives

$$\eta_l(u) = \sum_{k=0}^{\infty} E_{\tau,\theta} \{v_{2k}\} \mu_{\Omega}^{(2k)} \mu_R^{(2k)} u^{2k} \quad (28)$$

where  $\mu_{\Omega}^{(2k)} = E\{\Omega^{2k}\}$  and  $\mu_R^{(2k)} = E\{R^{2k}\}$ . For wireless channels, we evaluate  $E_{\tau_l, \theta_l}\{v_{2k}\}$  in (28) numerically by averaging uniformly over  $0 \leq \tau_l < 1$  and  $0 \leq \theta_l < 2\pi$ . After averaging the first  $M_N + M_D + 1$  terms of the infinite sum in (28), we only need to compute a single  $[M_N/M_D]$  PA,  $P_l(u)$ , as in (17) for each channel.

Under the assumption that each source's test statistic is independent including the gain, the phase and its first two derivatives, used to evaluate the  $P_e$  (14) and the saddle point, are

$$\Phi(u) = \sum_{l=0}^L \ln(P_l(u)) + \frac{1}{2} \sigma_w^2 u^2 - \ln u \quad (29)$$

$$\Phi'(u) = \sum_{l=0}^L \sum_{i=1}^{M_N} (u - z_{l,i})^{-1} - \sum_{j=1}^{M_D} (u - p_{l,j})^{-1} + \sigma_w^2 u - u^{-1} \quad (30)$$

$$\Phi''(u) = \sum_{l=0}^L - \sum_{i=1}^{M_N} (u - z_{l,i})^{-2} + \sum_{j=1}^{M_D} (u - p_{l,j})^{-2} + \sigma_w^2 + u^{-2}. \quad (31)$$

## 4.5 Padé Approximation Order

The PDF can be determined from the inverse Laplace transform of the MGF or its PA. In table 1, we evaluate the effectiveness of the PA by comparing the PDF at location  $x$  of a composite variate including Rayleigh fading and log-normal shadowing computed using Gauss-Laguerre (GL) integration,  $PDF_{GL}(x)$ , with the approximate PDF estimated from the corresponding PA,  $PDF_{PA}(x)$ . For the analysis, we set  $\sigma^2 = 1.0$  in (21) for the Rayleigh fading, and  $\mu_X = 0$  and  $\sigma_X^2 = 1$  in (19) for the log-normal shadowing. Defining the relative error,  $E_{Rel}(x)$ , as

$$E_{Rel}(x) = 100\% * |PDF_{GL}(x) - PDF_{PA}(x)| / PDF_{GL}(x), \quad (32)$$

the results from table 1 show that the maximum relative error for a [4/6] PA for the points evaluated is 0.10389% which is negligible. Increasing the PA order from [4/6] to [10/12] only decreases the maximum relative error for  $x = 3.6$  from 0.10389% to 0.10367%.

Next, we evaluated the performance of the SPI method using various PA orders by comparing the results to Monte Carlo simulations. In this analysis, we found that order [6/8] PAs are required to match the results from Monte Carlo simulations. For the case of Ricean fading channels without shadowing, a small increase in accuracy can be achieved in some scenarios by increasing the PA order to [10/12].

## 5 Numerical Results

In this section, we use the SPI method to evaluate the  $P_e$  for both ideal and wireless channels. In the figures, the value of  $E_b/N_0$  refers to the reference receiver and is defined to be

$$E_b/N_{0dB} = 10 \log_{10}(N^2 E\{\alpha_0^2\} a_0^2 / (2\sigma_w^2)) \quad (33)$$

with  $\sigma_w^2 = N_0/2$ . Without loss of generality, we choose to model equal transmitted powers and channel statistics for each of the sources. For the channel attenuation of ideal channels, we set  $\alpha_l = 1$ . For both Rayleigh and Ricean fading channels, the Gaussian variance used to compute the moments (22) is set to  $\sigma^2 = 0.5$ . For examples with fixed Rice factor,  $K$ , we choose  $K = 10 \log_{10}(s^2/(2\sigma^2)) = 6$  dB where  $s$  is the specular parameter given in (23). For macrocells, a typical value for the standard deviation associated with the log-normal shadowing is 8 dB [17]. For the following examples with fixed shadowing statistics, we set  $\sigma_{\Omega_l} = 8$  dB for each of the channels. For all wireless channel models, the numerator and denominator orders for the PAs are  $M_N = 6$  and  $M_D = 8$ . The error tolerances used for the numerical integration for ideal and wireless channels are 1e-9 and 1e-5, respectively.

First, we compare the  $P_e$  for all channel models while varying the numbers of sources and code lengths. In figure 2, we compare the results for code lengths of  $N = 31$  with  $L = 2$  MAI sources. Likewise, the results for code lengths of  $N = 511$  with  $L = 2$  and 10 MAI sources are given in figures 3 and 4, respectively. These results indicate that shadowing increases the  $P_e$  by a factor between 2 and 4 for Rayleigh channels and between 2 and 10 for Ricean channels. In each of the figures, the results for the wireless channels are all subject to an error floor. In figures 3 and 4, the  $P_e$  for ideal channels do not hit an error floor, while in figure 2, the  $P_e$  for the ideal channel is beginning to break towards an error floor. Since the MAI sources are all chosen to have transmitted powers equivalent to the reference source, the error floor is caused by multiple access interference dominating the  $P_e$  relative to the AWGN. Therefore, the  $P_e$  for ideal channels is more likely effected by the AWGN while the MAI contributes more significantly to the  $P_e$  for wireless channels.

Next, we compare the  $P_e$  results for asynchronous and synchronous chips for ideal channels, Rayleigh fading channels with shadowing and Ricean fading channels with shadowing. For rectangular chips, the  $P_e$  for synchronous chips is equivalent to the upper bound for asynchronous chips for the case of the reverse link. The error probability is greatest for syn-

chronous chips ( $\tau_l = 0$ ) because the cross-correlation between the reference and MAI chips, and therefore the interference, is maximized. This comparison is important because, when designing a wireless system, the system engineer must meet requirements for both average and upper bound error probabilities. In figure 5, we present results for  $L = 2$  MAI sources and  $N = 31$  random signature sequences. The error probabilities for  $N = 511$  random sequences and  $L = 2$  and 10 MAI sources are given in figures 6 and 7, respectively. Intuitively, one expects to observe a large difference in the average and upper bounds. For wireless channels, we observe that the error floors for synchronous chips are 2 to 10 times that of asynchronous chips at higher values of  $E_b/N_0$ . However, the difference is considerably less for the lower values of  $E_b/N_0$ . For ideal channels, we see from figure 5 that the  $P_e$  difference can be at least two orders of magnitude. For long code lengths and small numbers of MAI sources in figure 6, the average  $P_e$  and upper bound do not vary significantly for ideal channels. From these results, we see that the difference of the average  $P_e$  with the upper bound depends upon the contribution of the AWGN versus the MAI on the error probability. For both ideal and wireless channels, the difference is minor in the region of  $E_b/N_0$  where the AWGN dominates the  $P_e$  but becomes significant when the MAI is the major source of interference. In figure 6, the two curves for ideal channels are completely influenced by the AWGN and therefore almost identical. In figure 7 for ideal channels, the additional sources lead to a higher contribution of the MAI. As a result, we see that the difference between the average  $P_e$  and the upper bound for ideal channels is more significant when compared to figure 6. By reducing the code lengths from 511 to 31, the contribution of the MAI is even more pronounced leading to the largest difference in the average  $P_e$  and upper bound for ideal channels in figure 5. This result applies to wireless channels as well, but since the  $P_e$  is primarily affected by the MAI, the average  $P_e$  and the upper bound are similar only for lower values of  $E_b/N_0$ .

Since the SPI method is computationally efficient, it allows one to search various system

scenarios to locate specific operating points. For example, in figure 8 we determine the code lengths required to provide a  $P_e$  of 0.005 for a range of MAI sources. In order to ensure that we are considering the effects of the error floor only, all sources are operating with  $E_b/N_0 \rightarrow \infty$  dB. In the figure, we consider all channel combinations of Rayleigh and Ricean fading with and without shadowing. Given the increased  $P_e$  found in figures 2 through 4, it is not surprising the code lengths for the channels with shadowing must be 5 to 10 times longer than channels without shadowing to achieve a comparable error probability. It is also interesting to note that the curves are linear allowing one to infer code lengths required for larger numbers of MAI sources.

In figure 9, we compare the  $P_e$  versus  $L$  for  $N = 511$  chips as  $E_b/N_0 \rightarrow \infty$  dB. Again, we are comparing the error floors for the various system scenarios. The results indicate that increasing the number of MAI sources from 2 to 10 increases the  $P_e$  in the range from 5 to 10 for all channel models. However, for a domain of  $L = 10$  to 30, the  $P_e$  only increases by a factor of 2 to 5. From this figure, we also see that the effects of shadowing increase the  $P_e$  by a relatively constant value over a wide range of  $L$ . For Rayleigh fading, shadowing increases the  $P_e$  by 3.9 for  $L = 2$  and 3.0 for  $L = 30$ . Likewise, for Ricean fading, the increase in the  $P_e$  due to shadowing is 8.9 for  $L = 2$  and 8.8 for  $L = 30$ .

Instead of varying  $L$  for a fixed  $N$ , we next vary  $N$  for  $L = 10$  MAI sources as  $E_b/N_0 \rightarrow \infty$  dB in figure 10. For shorter code lengths, a small increase in  $N$  yields a large decrease in the  $P_e$ . For  $N \geq 350$ , we see only a minor improvement in the  $P_e$  for longer code lengths for all wireless channel models. Again, the increase in  $P_e$  due to shadowing is relatively constant over a large range of code lengths for both Rayleigh and Ricean fading.

In the last figure 11, we analyze the relationship between the standard deviation of the shadowing,  $\sigma_\Omega$ , and the  $P_e$  for channels with Ricean fading and varying values of the Rice factor  $K$ . In this example,  $N = 511$ ,  $L = 2$  MAI sources, and  $E_b/N_0 = 10$  dB. For macrocells and microcells, studies indicate that the shadowing  $\sigma_\Omega$  varies from 5 dB to 12 dB and 4 dB

to 13 dB, respectively [17]. From the figure, we observe that most of the changes in the  $P_e$  occur within these ranges of  $\sigma_\Omega$  values. For  $\sigma_\Omega < -5$  dB, the  $P_e$  approaches an asymptotic value equivalent to wireless channels which only exhibit fading. For  $\sigma_\Omega$  values greater than 13 dB, the receiver is operating very close to  $P_e = 0.5$ . For  $K = 10$  dB, the  $P_e$  increases by more than two orders of magnitude from  $\sigma_\Omega = -5$  dB to 13 dB. For the 4 - 13 dB  $\sigma_\Omega$  range, we see that the Rice factor  $K$  influences the  $P_e$  much less than for wireless channels modeled without shadowing ( $\sigma_\Omega < -5$  dB).

## 6 Conclusions

Evaluating error probabilities for DS/CDMA systems over wireless channels, which include the effects of shadowing and fading, is an extremely challenging mathematical task if approached directly using PDFs. However, using PAs based on the moment matching approach, we are able to develop a simple and computationally efficient solution by evaluating the contour integral of system's MGF. The fading and shadowing moments in the infinite series given in (16) grow exponentially. As a result, simply truncating the infinite series leads to large errors when evaluating the  $P_e$ . Using PAs eliminates this error by providing a rational approximation of the infinite sum. Including the effects of shadowing in the  $P_e$  simply involves multiplying individual fading moments by the shadowing moments before computing the PA. Results show that failure to account for the shadowing term typically results in an error in the  $P_e$  of 100% - 1000% but can be more than two orders of magnitude for channels with Ricean fading depending on the shadowing standard deviation and the Rice factor.

The SPI method for evaluating the  $P_e$  for DS/CDMA systems over both ideal and wireless channels proves to be efficient under both assumptions that all of the MAI sources are either chip-asynchronous or chip-synchronous with respect to the arrival of the reference signal at the receiver. Modeling chip-asynchronous, MAI sources occurs before evaluating the PA for

the system which only increases the processing time by a small percentage. From the results, the systems engineer can expect the  $P_e$  to increase by a factor ranging between 2 to 10 when comparing the average  $P_e$  to the worst-case  $P_e$  under the assumption of rectangular chips.

The near-far problem occurs in the reverse link where the higher received powers from the MSs which are closer to the BS cause higher probabilities of error for the MSs which are located further away in the cell. In cellular DS/CDMA, fast Transmission Power Control (TPC) combats the near-far problem by controlling the transmit power for each of the MSs so that the received powers at the BS for each MS are approximately equal. Given that neither open-loop or closed-loop TPC can produce equal received powers for the MSs at the BS, TPC minimizes the effects of distance, shadowing, and fading. For shadowing and fading, TPC reduces the *variances* of these effects so that the true  $P_e$  will be somewhere between the results for ideal channels and wireless channels presented in this paper for both cases of fading only and fading with shadowing. Thus, the SPI method can be used to analyze the contribution of the TPC errors on the  $P_e$  in the case of shadowing by using results similar to those found in figure 11. For the particular scenario presented in the figure, we can evaluate the effects of the TPC error on the  $P_e$  for a given shadowing standard deviation resulting from misestimating the shadowing effect.

Finally in some wireless systems, TPC may not be practical or even desired. For example in a battle field communications system, it may not be desired for a base station to continuously transmit for the sole purpose of power control thereby giving away its location. Also, TPC may not be an option in Industrial, Scientific, and Medical (ISM) bands where multiple, independent DS/CDMA networks could be operating simultaneously. TPC may be used for one sub-network, but the other sub-networks will be producing uncontrolled interference. Moreover, TPC does not work in peer-to-peer networks such as two- or three-way, walkie-talkie systems in a crowded event where, again, multiple sub-networks are operating independently. Therefore, the system designer should take into account the effects of shad-

owing when analyzing the system  $P_e$ , and the SPI method can be used to model shadowing in a wireless network.

## References

- [1] H. Amindavar and J.A. Ritcey, "Padé Approximations of Probability Density Functions", IEEE Trans. Aero. and Elect. Sys., AES-30, 2, April 1994, pp. 416-424.
- [2] H. Amindavar and J.A. Ritcey, "Padé Approximations for Detectability in K-Clutter and Noise", IEEE Trans. Aero. and Elect. Sys., AES-30, 2, April 1994, pp. 425-434.
- [3] E.A. Geraniotis and M.B. Pursley, "Error Probability for Direct-Sequence, Spread-Spectrum Multiple-Access Communications - Part II: Approximations", IEEE Trans. on Communications, COM-30, 5, May 1982, pp. 985-995.
- [4] E.A. Geraniotis and M.B. Pursley, "Performance of Coherent Direct-Sequence, Spread-Spectrum Communications over Specular Multipath Fading Channels", IEEE Trans. on Communications, COM-33, 6, June 1985, pp. 502-508.
- [5] S. Gordon and J.A. Ritcey, "Calculating the K-Distribution by Saddlepoint Integration", IEE Proc.-Radar, Sonar, Navig, 142, 4, Aug. 1995, pp. 162-166.
- [6] C.W. Helstrom, "Calculating Error Probabilities for Intersymbol and Cochannel Interference", IEEE Trans. on Communications, COM-34, May 1986, pp. 430-435.
- [7] C.W. Helstrom and J.A. Ritcey, "Evaluating Radar Detection Probabilities by Steepest Descent Integration", IEEE Trans. Aero. and Elect. Sys., AES-20, 5, Sept. 1984, pp. 624-633.
- [8] C.W. Helstrom, Elements of Signal Detection & Estimation, Prentice Hall, Englewood Cliffs, NJ, 1995, Appendix C, p. 524.
- [9] P. Henrici, Applied and Computational Complex Analysis, vol. 1, John Wiley and Sons, New York, NY, 1974, p. 42.
- [10] K.S. Kim, S.Y. Kim, S.C. Kim, and I. Song, "Design and Analysis of Concatenated Coded DS/CDMA Systems in Asynchronous Channels", IEEE Trans. Veh. Tech., 48, 5, Sept. 1999, pp. 1421-1427.
- [11] K.S. Kim, I. Song, Y.H. Kim, Y.U. Lee, and J. Lee, "Analysis of Quasi-ML Multiuser Detection of DS/CDMA Systems in Asynchronous Channels", IEEE Trans. on Communications, COM-47, 12, Dec. 1999, pp. 1875-1883.
- [12] K.S. Kim, I. Song, H.G. Kim, Y.H. Kim, and S.Y. Kim, "A Multiuser Receiver for Trellis-Coded DS/CDMA Systems in Asynchronous Channels", IEEE Trans. Veh. Tech., 49, 3, May 2000, pp. 844-855.
- [13] J.S. Lehnert and M.B. Pursley, "Error Probabilities for Binary Direct-Sequence Spread-Spectrum Communications with Random Signature Sequences", IEEE Trans. on Communications, COM-35, 1, Jan. 1987, pp. 87-97.

- [14] M.B. Pursley, "Performance Evaluation for Phase-Coded Spread-Spectrum Multiple-Access Communications - Part I: System analysis", IEEE Trans. on Communications, COM-25, 8, Aug. 1977, pp. 795-799.
- [15] S.O. Rice, "Efficient Evaluation of Integrals of Analytic Functions by the Trapezoidal Rule", Bell System Technical Journal, 52, May-June 1973, pp. 707-723.
- [16] J.S. Sadowsky and R.K. Bahr, "Direct-Sequence Spread-Spectrum Multiple-Access Communications with Random Signature Sequences: A Large Deviations Analysis", IEEE Trans. on Information Theory, IT-37, 3, May 1991, pp. 514-526.
- [17] G.L. Stüber, Principles of Mobile Communications, Kluwer Academic Publishers, Norwell, Massachusetts, 1996, Chapter 2, pp. 35-90.
- [18] M.O. Sunay and P.J. McLane, "Sensitivity of a DS CDMA System with Long PN Sequences to Synchronization Errors", Proceedings ICC'95, Seattle, WA, 2, June 18-22, 1995, pp. 1029-1035.

$x$	$PDF_{GL}(x)$	$PDF_{PA}(x)$	$E_{Rel}(x)$
0.4	3.9891e-1	3.9894e-1	0.00885
0.8	5.8473e-1	5.8493e-1	0.03452
1.2	5.4469e-1	5.4474e-1	0.01004
1.6	3.9814e-1	3.9794e-1	0.05065
2.0	2.4934e-1	2.4923e-1	0.04370
2.4	1.4075e-1	1.4083e-1	0.05555
2.8	7.4146e-2	7.4206e-2	0.08147
3.2	3.7297e-2	3.7285e-2	0.03230
3.6	1.8162e-2	1.8143e-2	0.10389
4.0	8.6441e-3	8.6429e-3	0.01429

Table 1: Comparison of the relative error for a composite PDF with Rayleigh fading and log-normal shadowing using Gauss-Laguerre integration and a [4/6] Padé approximation model.

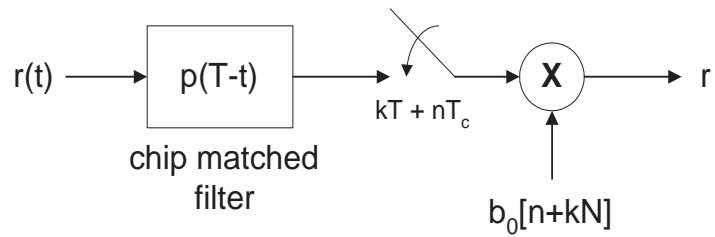


Figure 1: Reference Receiver Model.

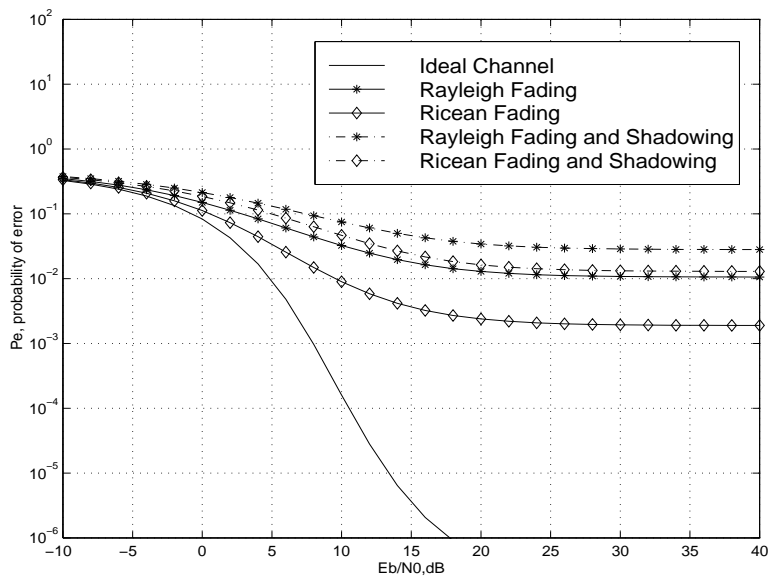


Figure 2:  $P_e$  vs.  $E_b/N_0$  for  $L = 2$  MAI sources, and  $N = 31$ . Channel models include ideal, Rayleigh fading with and without shadowing, and Ricean fading with and without shadowing.

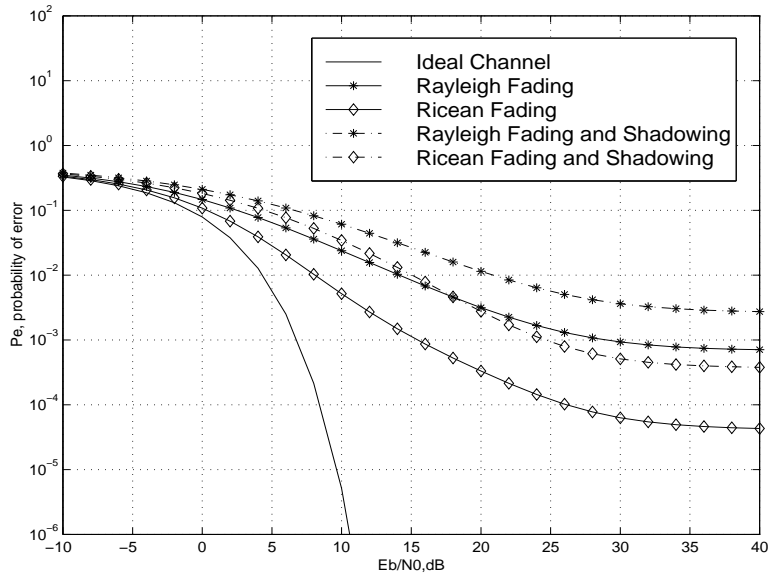


Figure 3:  $P_e$  vs.  $E_b/N_0$  for  $L = 2$  MAI sources, and  $N = 511$ . Channel models include ideal, Rayleigh fading with and without shadowing, and Ricean fading with and without shadowing.

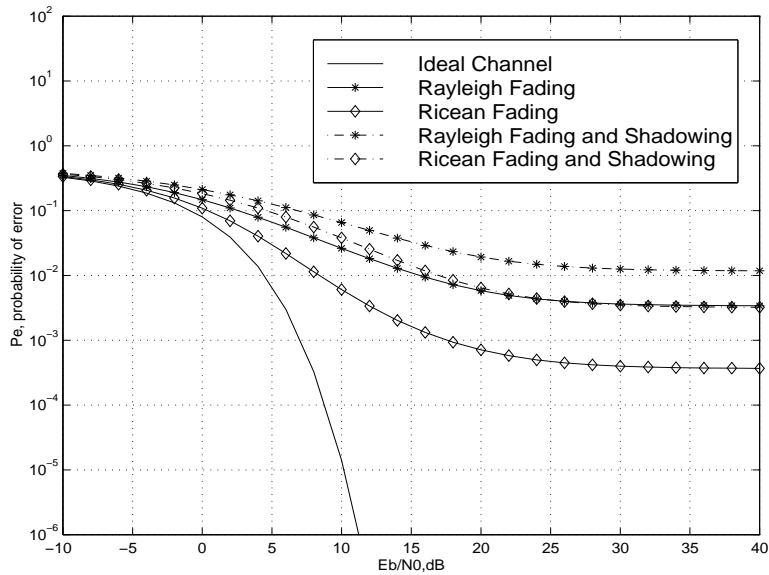


Figure 4:  $P_e$  vs.  $E_b/N_0$  for  $L = 10$  MAI sources, and  $N = 511$ . Channel models include ideal, Rayleigh fading with and without shadowing, and Ricean fading with and without shadowing.

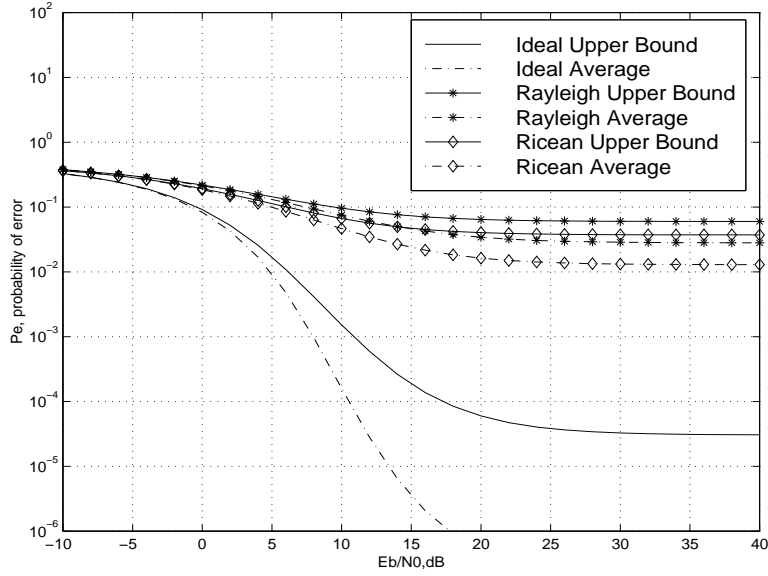


Figure 5: Comparison of average and worst case  $P_e$  vs.  $E_b/N_0$  for  $L = 2$  MAI sources and  $N = 31$  random signature sequences. Average  $P_e$  corresponds to asynchronous, rectangular chips and worst case  $P_e$  applies to synchronous, rectangular chips. All wireless channels include shadowing.

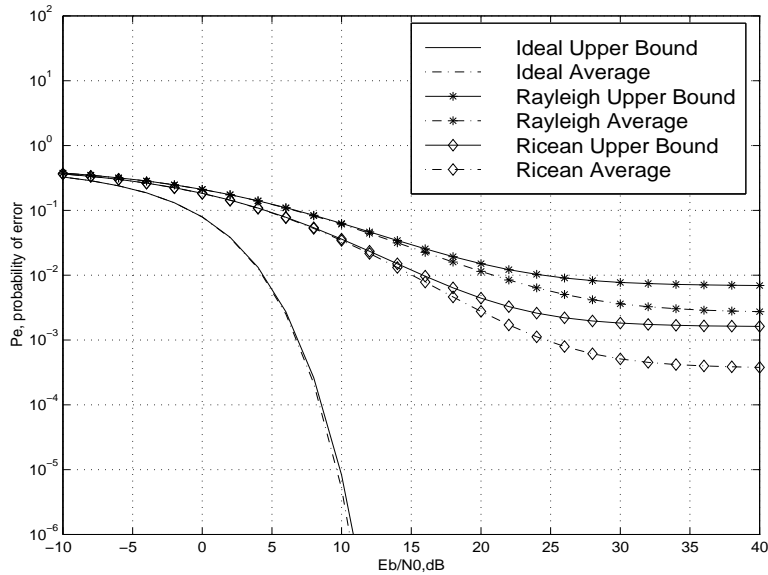


Figure 6: Comparison of average and worst case  $P_e$  vs.  $E_b/N_0$  for  $L = 2$  MAI sources and  $N = 511$  random signature sequences. Average  $P_e$  corresponds to asynchronous, rectangular chips and worst case  $P_e$  applies to synchronous, rectangular chips. All wireless channels include shadowing.

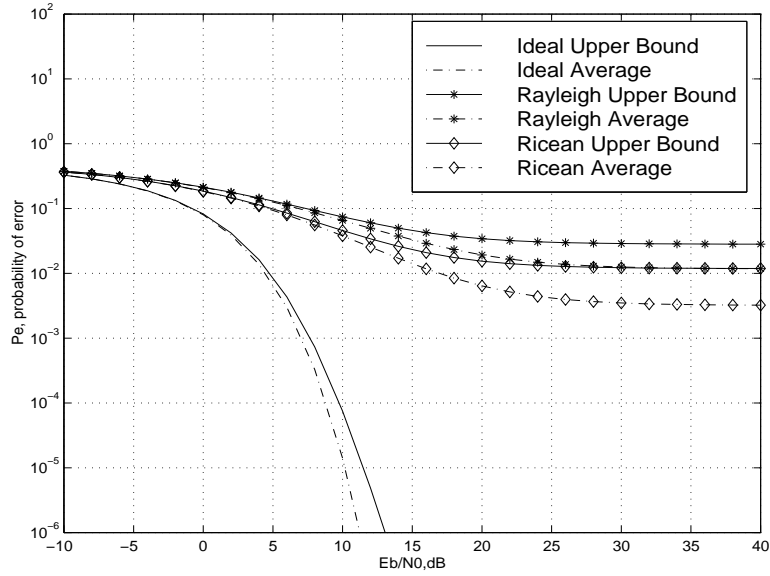


Figure 7: Comparison of average and worst case  $P_e$  vs.  $E_b/N_0$  for  $L = 10$  MAI sources and  $N = 511$  random signature sequences. Average  $P_e$  corresponds to asynchronous, rectangular chips and worst case  $P_e$  applies to synchronous, rectangular chips. All wireless channels include shadowing.

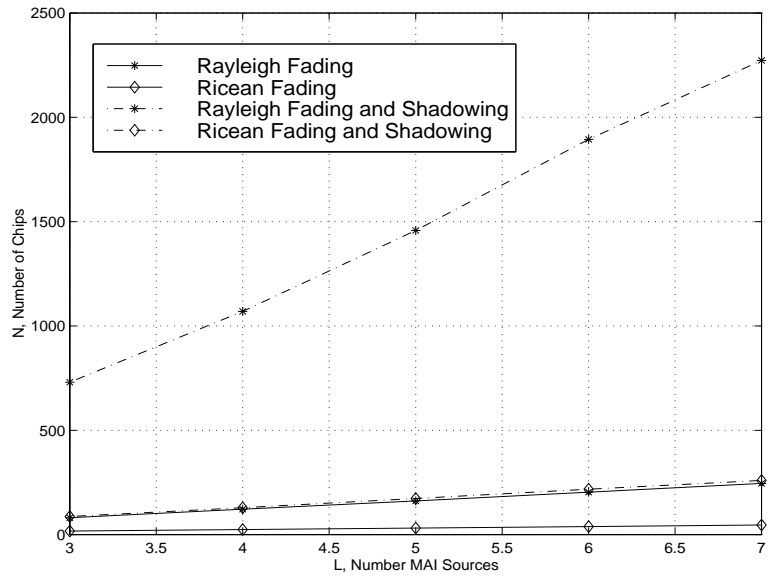


Figure 8:  $N$  vs.  $L$  for wireless channels operating at  $P_e = 0.005$  for  $E_b/N_0 \rightarrow \infty$  dB.

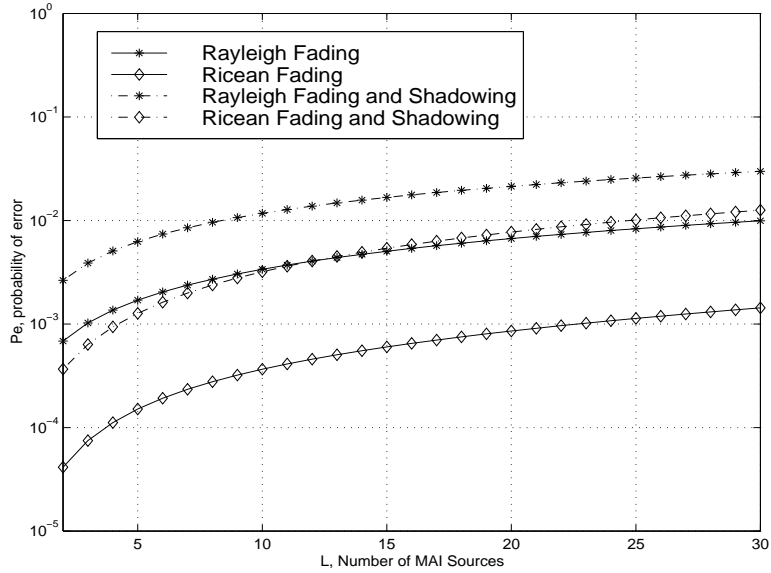


Figure 9:  $P_e$  vs.  $L$  for wireless channels and a code length,  $N = 511$ .

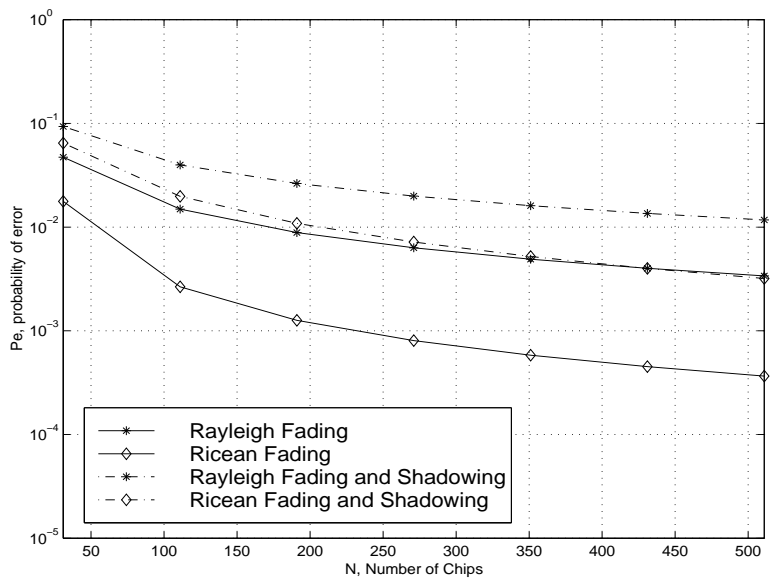


Figure 10:  $P_e$  vs.  $N$  for wireless channels and  $L = 10$  MAI sources.

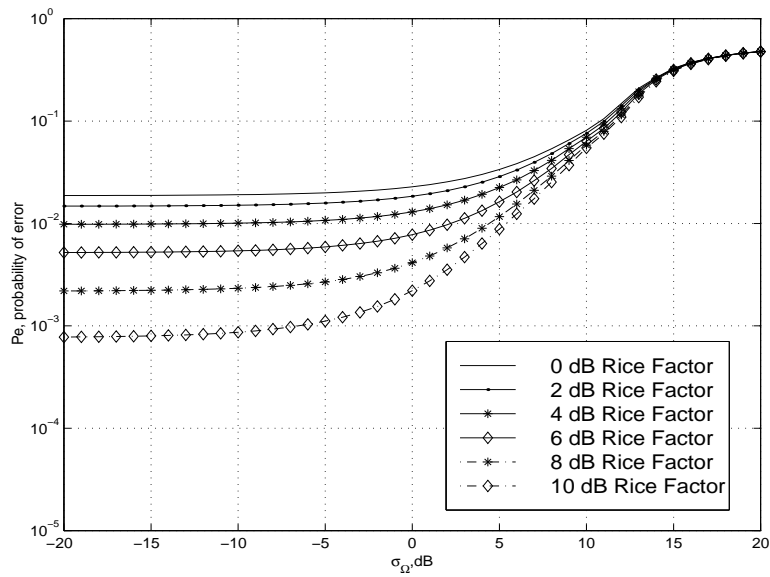


Figure 11:  $P_e$  vs. shadowing standard deviation for various Rice factors,  $L = 2$  MAI sources, and  $E_b/N_0 = 10$  dB.